ORIGINAL PAPER

Multiscale molecular dynamics simulations of sodium dodecyl sulfate micelles: from coarse-grained to all-atom resolution

**Guillaume Roussel · Catherine Michaux ·
Eric A. Perpète**

Abstract Sodium dodecyl sulfate (SDS) is a well-known anionic detergent widely used in both experimental and theoretical investigations. Many molecular dynamics (MD) simulation have been performed on the SDS molecule at coarse-grained (CG), united-atom (UA), and all-atom (AA) resolutions. However, these simulations are usually based on general parameters determined from large sets of molecules, and as a result, peculiar molecular specificities are often poorly represented. In addition, the parameters (ideal bond lengths, angles, dihedrals and charge distribution) differ according to the resolution, highlighting a lack of coherence. We therefore propose a new set of parameters for CG, UA, and AA resolutions based on a high quantum mechanics (QM) level optimization of the detergent structure and the charge distribution. For the first time, QM-optimized parameters were directly applied to build the AA, UA, and CG model of the SDS molecule, leading to a more coherent description. As a test case, MD simulations were then performed on SDS preformed micelles as previous experimental and theoretical investigations allow direct comparison with our new sets of parameters. While all three models yield similar macromolecular properties (size, shape, and accessible surface) perfectly matching previous results, the attribution of more coherent parameters to SDS enables the description of the specific interactions inside and outside the micelle. These more consistent parameters can now be used to accurately describe new multi-scale systems involving the SDS molecule.

G. Roussel (✉) · C. Michaux · E. A. Perpète
Unité de Chimie Physique Théorique et Structurale (UCPTS),
University of Namur, Rue de Bruxelles, 61, 5000 Namur, Belgium
e-mail: guillaume.roussel@unamur.be

Introduction

Sodium dodecyl sulfate (SDS) is a well-known anionic detergent widely used in both experimental and theoretical investigations such as SDS-protein interactions [1–5] or detergent micellization itself. Indeed, many experimental studies have been performed to determine the size and shape of SDS micelles, as well as their aggregation number [6–10], the dynamics of the hydrocarbon chains [11–13], or the solvent penetration within the hydrophobic inner core [14, 15]. However, the interpretation of experimental results is often model-dependent, making theoretical studies of micelles a crucial stage to obtain relevant molecular pictures. Molecular dynamics (MD) simulations on SDS micelles have therefore been performed at the coarse-grained (CG) [16–19], united-atom (UA) [20–24], and all-atom (AA) [25–27] resolutions. However, the limitations of the method are related to the description of the molecule at each resolution (ideal bond lengths, angles, dihedrals, and partial charges distribution) [28] that usually remains based on general parameter sets covering wide areas of biochemistry [29] and therefore missing the specificity of the newly investigated systems. Moreover, multiscale simulations [30–32] are currently performed using parameters sets that differ according to the resolution. Indeed, while the charge is exclusively carried by the polar headgroup for the CG representation [16], the UA model displays a non-negligible charge on the first methyl group (C1; Table 1; reference) of the hydrocarbon tail [20], and this charge is distributed along the whole molecule for the AA model [25]. As a consequence, a more coherent set of parameters for the SDS molecule at CG, UA, and AA resolutions is needed to circumvent this major MD drawback.

We here propose to describe (partial charges, ideal bond lengths, angles, and dihedrals) the SDS molecule for each resolution starting from a QM-optimized model. Doing so, and for the first time, the corresponding parameters will be in

Table 1 Partial charges (e) for the SDS molecule at all-atom (AA), united-atom (UA), and coarse-grained (CG) resolutions

	Coherent models			Reference		
	AA	UA	CG	AA [20]	UA [15]	CG [11]
OM	−0.618	−0.618	−1.203	−0.633	−0.654	−1.000
OM	−0.618	−0.618		−0.633	−0.654	
OM'	−0.601	−0.601		−0.633	−0.654	
S	+1.105	+1.105		+1.256	+1.284	
OA	−0.471	−0.471		−0.528	−0459	
C1	+0.259	+0.245	+0.233	+0.370	+0.137	0.000
H1.1	−0.007			−0.035		
H1.2	−0.007			−0.035		
C2	+0.061	+0.039		+0.116	0.000	
H2.1	−0.011			−0.031		
H2.2	−0.011			−0.031		
C3	−0.064	−0.092		−0.095	0.000	
H3.1	−0.014			−0.019		
H3.2	−0.014			−0.019		
C4	+0.139	+0.041		+0.251	0.000	
H4.1	−0.049			−0.078		
H4.2	−0.049			−0.078		
C5	+0.101	+0.029	+0.030	+0.055	0.000	0.000
H5.1	−0.036			−0.036		
H5.2	+0.036			−0.036		
C6	−0.053	−0.071		+0.031	0.000	
H6.1	−0.009			−0.033		
H6.2	−0.009			−0.033		
C7	+0.076	+0.018		+0.053	0.000	
H7.1	−0.029			−0.034		
H7.2	−0.029			−0.034		
C8	−0.132	+0.054		+0.217	0.000	
H8.1	−0.039			−0.065		
H8.2	−0.039			−0.065		
C9	−0.084	−0.085	−0.060	−0.088	0.000	0.000
H9.1	−0.001			−0.011		
H9.2	−0.001			−0.011		
C10	+0.038	+0.006		+0.099	0.000	
H10.1	−0.046			−0.036		
H10.2	−0.046			−0.036		
C11	+0.233	+0.131		+0.224	0.000	
H11.1	−0.016			−0.054		
H11.2	−0.016			−0.054		
C12	−0.281	−0.112		−0.224	0.000	
H12.1	+0.055			+0.043		
H12.2	+0.055			+0.043		
H12.3	+0.059			+0.047		

the description of the molecules by integrating a large number of degrees of freedom into a handful of entities: a hydrophilic group (including all the atoms of the headgroup) bearing a negative charge, and three hydrophobic beads (each representing four methylene groups [16]) (Fig. 1c).

Thanks to the previous experimental and theoretical investigations, we were able to check the relevance and accuracy of these three original models in describing the dynamic behavior of preformed micelles in water. These coherent sets of AA, UA, and CG parameters could now be used to investigate the SDS-protein interactions at multiscale resolutions.

Methods

QM-based SDS parameters

The geometry of a single SDS molecule was optimized with the Gaussian 09 package at the B3LYP/6-311++G(2d,2p) level which has proved to yield reliable structural parameters [33–35], and the atom charges were computed using the electrostatic potential charges (ESP) that have been very efficient and successfully applied for a variety of systems [33, 36]. For the AA model, the existing atom types and force constants reported for the gromos53a5 forcefield [29] were used, and the QM obtained partial charges were attributed to each atom as listed in Table 1. Equilibrium bond lengths, angles, and dihedrals were derived from the optimized structure. As for AA model, the UA detergent molecule was built by using existing united-atom types and force constant from the gromos53a5 forcefield. United-atom charges were obtained by summarizing the charges from all atoms of the methyl group into a single point as shown in Table 1. Finally, the CG structure was obtained using the MARTINI forcefield [37] with the corresponding parameters for SDS set as previously described [16] except for the partial charges, obtained by summing the charges derived from the QM-optimized model into the relevant coarse-grained groups [38] (see Table 1).

Simulated systems

The SDS micelles were built using Packmol [39] by assembling 60 SDS molecules to match an experimental aggregation number in the range of 55–70 [6–8] as well as the number of monomers previously described in other theoretical investigations [16, 20, 24]. The terminal carbon beads (CG) or atoms (AT and AA) were placed inside a virtual sphere of 3.5 Å while the hydrophilic bead (CG) or the sulfur atom (UA and AA) was located outside a second virtual sphere with a radius of 16 Å. All the preformed micelles were then placed in a cubic simulation box which was subsequently filled with 20,000 single-point-charge (SPC) water molecules, for a final SDS concentration of 150 mM. To ensure the charge

line for the three resolutions: (i) the AA model taking into account the 42 atoms of the molecule (Fig. 1a); (ii) an UA model reducing the number of degrees of freedom by merging each methyl group pertaining to the hydrocarbon tail into a unique particle (Fig. 1b); (iii) a CG model further simplifying

Fig. 1 Structure of sodium dodecyl sulfate at the all-atom (AA), united-atom (UA), and coarse-grained (CG) resolutions. Carbon atoms are numbered according to their position within the hydrophobic tail
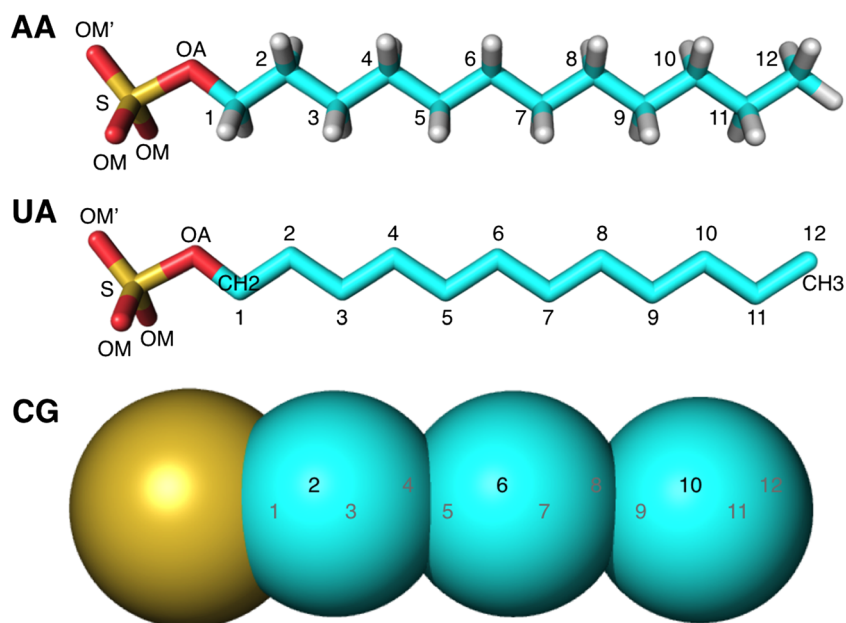
neutrality, 60 Na$^+$ ions were introduced by randomly replacing water molecules.

Details of the simulations

All simulations were completed using the GROMACS 4.5.5 version [40]. The energy of the initial configuration was minimized with the steepest descent method, which is known to give adequate configurations for similar systems [20, 41]. Next, all simulations were performed in the NPT ensemble. For all AA, UA, and CG models, SDS and water molecules were separately coupled to a Berendsen thermostat [42] at 293.15 K and the barostat set was at 1 bar to match the experimental conditions. A timestep of 2 fs was applied for both AA and UA models, and 40 fs for the CG model. Analyses were performed by using the GROMACS tools, while VMD [43] and Pymol (The PyMOL Molecular Graphics System, Version 1.5.0.4 Schrödinger, LLC.) were used for visualization.

Results and discussion

After comparing the QM-derived parameters of SDS with those commonly used for MD simulations, we present the modelled SDS micelle according to three properties: (i) the general outer SDS structure corresponding to the size and the shape of the micelle; (ii) the inner SDS structure involving the distribution of chemical groups along the micelle axis and the interactions of hydrophobic tails with water molecules; and (iii) the specific interactions occurring at the surface of the micelle.

Electronic and structural parameters of SDS molecule

The partial charge distributions and the structural parameters derived from the QM-optimized molecule at the three resolutions are listed in Tables 1 and 2 respectively. Slight differences are observed on the charge distribution between our AA model and the previously proposed model [25], most probably due to the selected QM optimization level selected (B3LYP/6-311++G(2d,2p) versus B3LYP/6-31+G(d) [25]). However, even if the net charge over the alkyl tail (from C2 to C12) is weak for both models (−0.042 e according to our optimization and −0.040 for Yan et al.), there are non-negligible values at the end of the hydrophobic tail. For instance, in both models, C11 and C12 carry charges of +0.233 and −0.281 e (+0.224 and −0.244 previously), respectively (Table 1), that could slightly affect the interactions with other molecules.

We then set up new UA and CG models derived from the AA model by summing the charges from all atoms of one or four methyl group(s) into a single point for the UA or CG molecules respectively. In comparison to the three reference models (Table 1, right), our newly described SDS molecule shows different charge values and a more coherent distribution of them between the three different resolutions (Table 1, left). Indeed, while partial charges of each methyl group are set to zero in the UA and CG reference models, our UA and CG molecules display a value corresponding to the sum of the charges on each atom constituting the particle, leading to a more coherent description of the system.
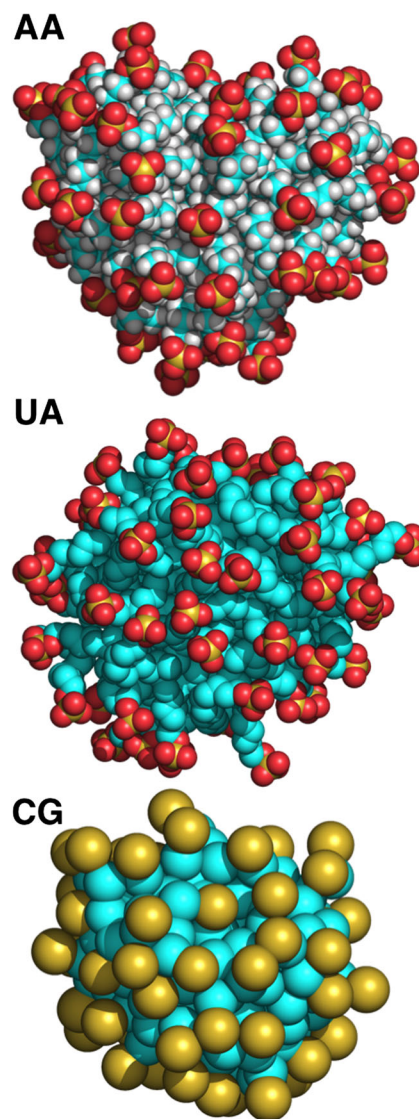
The micelle outer structure

For each model, the preassembled micelle (60 SDS molecules) remains stable throughout the course of the entire

Table 2 Bond lengths, angles, and dihedrals parameters for SDS molecule at all-atom (AA) and united-atom (UA) resolution

	QM-based models		References	
	AA	UA	AA [25]	UA [21]
a. Bond length (nm)				
OM-S	0.147	0.147	0.145	0.150
OM'-S	0.146	0.146	0.144	0.150
S-OA	0.170	0.170	0.163	0.136
OA-C1	0.142	0.142	0.140	0.143
C1-C2	0.152	0.152	0.152	0.152
C-C	0.153	0.153	0.153	0.152
C-H	0.109	N.A.	0.109	N.A.
b. Angles (deg)				
OM-S-OM	115.6	115.6	113.6	119.0
OM-S-OM'	114.0	114.0	115.1	119.0
OM-S-OA	104.3	104.3	104.5	105.0
OM'-S-OA	100.6	100.6	102.1	105.0
S-OA-C	114.4	114.4	117.1	120.0
OA-C-C	108.2	108.2	107.8	115.0
C(H2)-C(H2)-C(H2)	113.8	113.8	113.4	111.0
C(H2)-C(H2)-C(H3)	113.4	113.4	113.1	111.0
OA-C-H	109.9	N.A.	109.6	N.A.
H-C(H2)-H	105.9	N.A.	106.2	N.A.
H-C(H3)-H	107.6	N.A.	107.6	N.A.
H-C(H2)-C(H2)	109.0	N.A.	109.3	N.A.
H-C(H3)-H	111.3	N.A.	111.3	N.A.
c. dihedrals (deg)				
OM'-S-OA-C	180.0	180.0	180.0	180.0
OM-S-OA-C	59.9	59.9	59.9	60.0
S-OA-C-C	180.0	180.0	180.0	180.0
OA-C-C-C	180.0	180.0	180.0	180.0
S-OA-C-H	59.3	N.A.	59.4	N.A.
OA-C-C-H	57.9	N.A.	57.9	N.A.
C-C-C(H2)-H	57.7	N.A.	57.8	N.A.
C-C-C(H3)-H	59.8	N.A.	59.9	N.A.

Fig. 2 Final all-atom (AA), united-atom (UA), coarse-grained (CG) micelles at the end of the production run. Headgroups are in red or orange while hydrophobic tails are in cyan

20 ns run, and snapshots of the AA, UA, and CG micelles at the end of the production runs are presented in Fig. 2.

As a typical descriptor, the average radius of gyration (Rg) is used to characterize the micelles, and we obtained values of 16.8±0.6, 16.8±0.5, and 15.5±0.2 Å for the AA, UA, and CG models, respectively. The effective micelle radius (R$_s$), which can be compared to experimental results, were determined by using the equation based on the relationship between the radius of a sphere of uniform density and its R$_g$ as previously described [44]. The R$_s$ values correspond to 21.7±0.8, 21.7± 0.7, and 20.0±0.2 Å for the three models (Table 3). All of them give values in good agreement with the experimental results obtained by neutron scattering (19.5±1.4 Å [8]), dynamic light scattering (22.1±1.1 Å [10]), and X-ray scattering (22.3±1.2 Å [12]), and they also match previous MD simulations [16, 20, 21, 45]. Remarkably, explicitly taking hydrogen atoms into account does not significantly redimension the structure, as AA and UA micelles have similar sizes.

To describe the evolution of the micelle shape starting from a perfect sphere, the principal moments of inertia (I$_1$, I$_2$, and I$_3$) and the eccentricity (e) were computed (Table 3). For each micelle, the eccentricity evolves from zero for a perfect sphere to 1 for a "rod-like" object [46]. The values of 0.17±0.06, 0.18±0.08, and 0.17±0.06 for AA, UA, and CG models indicate that, whatever the model, the micelles show a prolate ellipsoidal shape matching previous theoretical and experimental investigations [11, 16, 23, 24, 26, 47].

Finally, the solvent accessible surface area (SAS) allows a characterization of the interactions between the micelle and the surroundings. The total SAS of the relaxed micelles are

Table 3 Characterization of the outer structure of the all-atom (AA), united-atom (UA), and coarse-grained (CG) micelle. R_g: radius of gyration. R_s: micelle radius. I_i: moment of inertia. e: eccentricity. SAS: solvent accessible surface area

	Rg (Å)	Rs (Å)	I_1	I_2	I_3	e	SAS (Å²) hydrocarbon tails	SAS (Å²) headgroups	SAS (Å²) total
AA	16.8±0.6	21.6±0.8	1.00±0.05	1.23±0.07	0.39±0.07	0.17±0.06	4533±245	6637±191	11170±371
UA	16.8±0.5	21.7±0.7	1.00±0.06	1.26±0.08	140±0.09	0.18±0.08	4245±230	6516±131	10761±355
CG	15.5±0.2	20.0±0.2	1.00±0.05	1.23±0.06	1.39±0.07	0.17±0.06	3489±206	6797±204	10286±327

11,170±371, 10,761±355, and 10,286±327 Å² for the AA, UA, and CG models (Table 3) corresponding to 186.2±6.2, 179.4±5.9, and 171.4±5.5 Å² of SAS per monomer, respectively.

In summary, whatever the resolution, the SDS micelle's macromolecular properties are well in line with previous experimental and theoretical results, validating our systematically QM-derived sets of parameters.

The micelle inner structure

The inner micelle structure can be analyzed in terms of radial distribution of the different groups constituting the system, i.e., the hydrocarbon tails, the headgroups, the sodium ions, and the

water molecules (Fig. 3). For all three resolutions, the distributions show similar overall trends. As expected, the hydrocarbon tails (black curve) are maintained inside the micelle, constituting the so-called hydrophobic core. Similarly, the maximum for the tails distribution is distant by 10 Å from the center of mass (COM; black dashed line). The headgroups (red line) are distributed around the hydrophobic core with a peak at 18 Å, followed by the sodium counterions at 20 Å (green curve), consistent with previous results [8, 12, 16, 22, 26].

There are no water molecules (blue line) within 12 Å to the COM indicating that up to this limit the inside of the micelle is totally water-free (see scheme on Fig. 6). As a result, there is a significant overlap region (from 12 to 23 Å to the COM) in which the aliphatic tail and water molecules can be in contact.
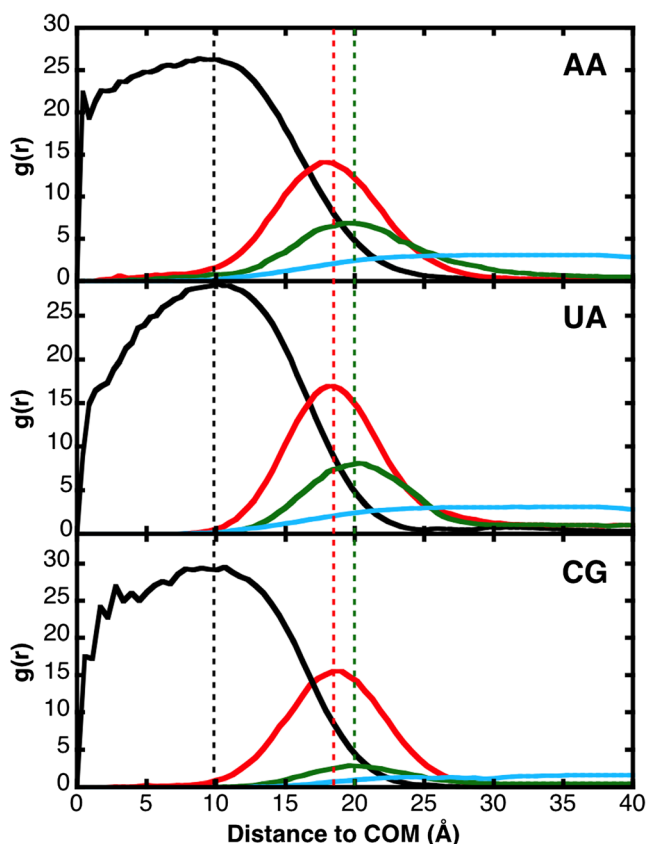

Fig. 3 Radial distribution in terms of the distance from the micelle center of mass (COM) of the hydrocarbon tails (black), headgroups (red), sodium ions (green), and water molecules (blue) at all-atom (AA), united-atom (UA), and coarse-grained (CG) resolutions
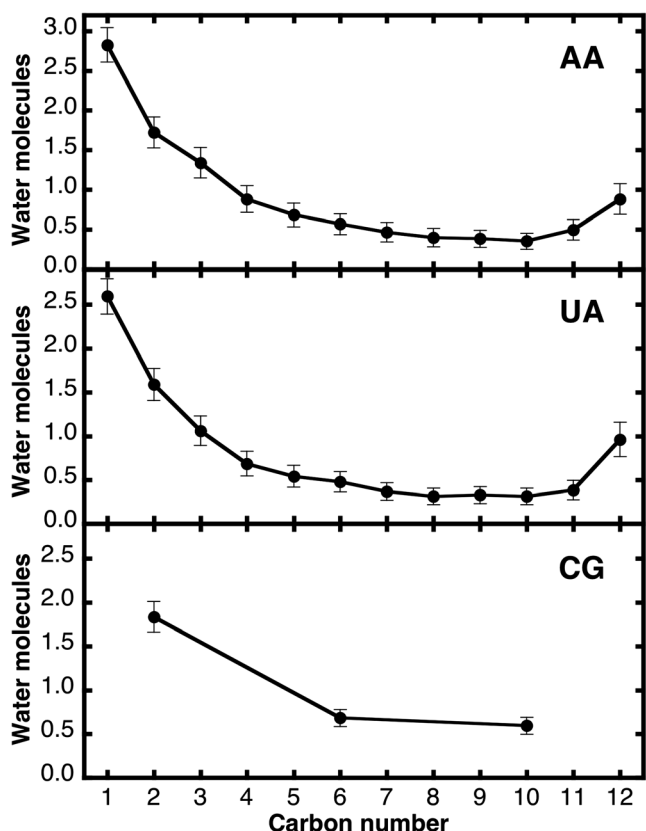
Fig. 4 Number of water molecules neighboring the carbon atoms constituting the hydrophobic tail in the all-atom (AA), united-atom (UA), and coarse-grained (CG) models. Carbon number refers to the position in the tail as depicted in Fig. 1
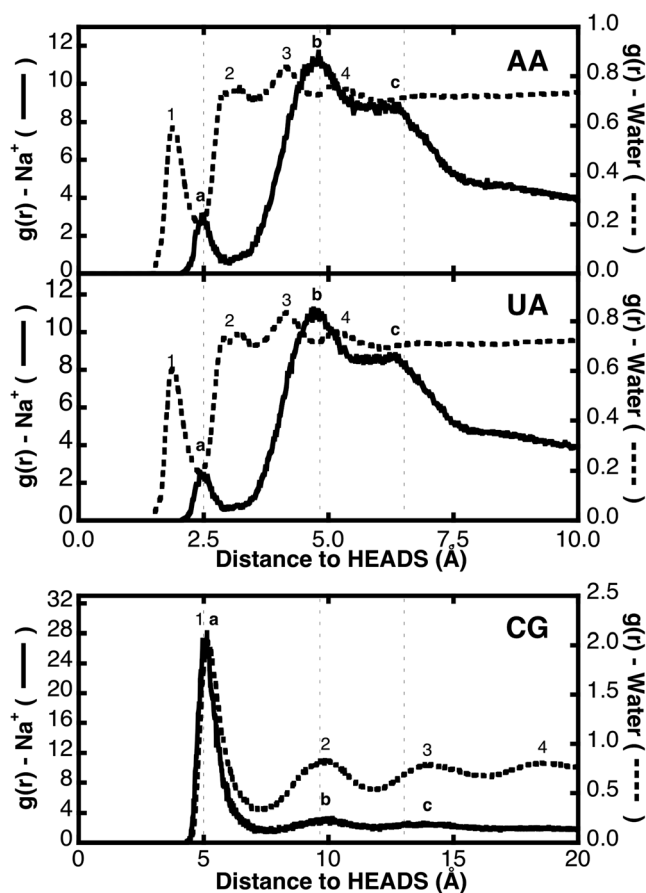
Fig. 5 Radial distribution functions between the sulfate headgroups and water molecules (dashed line) or sodium ions (bold line) for the all-atom (AA), united-atom (UA), and coarse-grained (CG) models

Again, this is in line with previously published data [8, 11, 13, 20, 21, 24, 48].

The ability of the hydrocarbon subunits to be surrounded by water molecules has subsequently been evaluated. For each carbon constituting the detergent tail (from C1 to C12; see carbon numbering on Fig. 1), the number of water molecules neighboring each carbon atom by less than 3.5 Å is reported in Fig. 4. It decreases when going from C1 to C5 and reaches values close to zero for C6–C11. The non-negligible values for the four first carbon atoms indicate that headgroups do not completely cover the micelle surface (as observed on Fig. 2), allowing some water-hydrocarbon contacts, as also observed from the calculated hydrocarbon tails SAS (Table 3). From C6, the hydrophobic tail is fully embedded inside the micelle and is consequently protected from water molecules. However, few water molecules are observed around the terminus carbon atom (Fig. 4, C12; not observed on the CG model due to the low resolution) indicating some exposure of the C12 methyl group outside the water-free region (see Fig. 6, arrows) as previously mentioned from MD simulations [26] and experiments [15].

In agreement with previous experimental and theoretical studies, the three levels of approximation lead to the consistent organization of the inner part of the micelle.

The micelle-bulk interface

Finally, we investigated the micelle-bulk interface by calculating the radial distribution function of the headgroup-salt or headgroup-water association (Fig. 5). The CG model clearly differs from the UA and AA's, as it results in an overlap of the water molecules distribution with the sodium ions. For both AA and UA models, a first peak is observed around 1.9 Å corresponding to a first hydration shell (dashed line) exclusively consisting of water molecules solvating the non-charged oxygen of the detergent, as previously mentioned [21, 26]. Then, two major peaks

Fig. 6 United-atom micelle cross section at the end of the production run. Atoms are represented by the following colors: cyan = carbon; red = oxygen; yellow = sulfur; white = hydrogen; blue = sodium ion
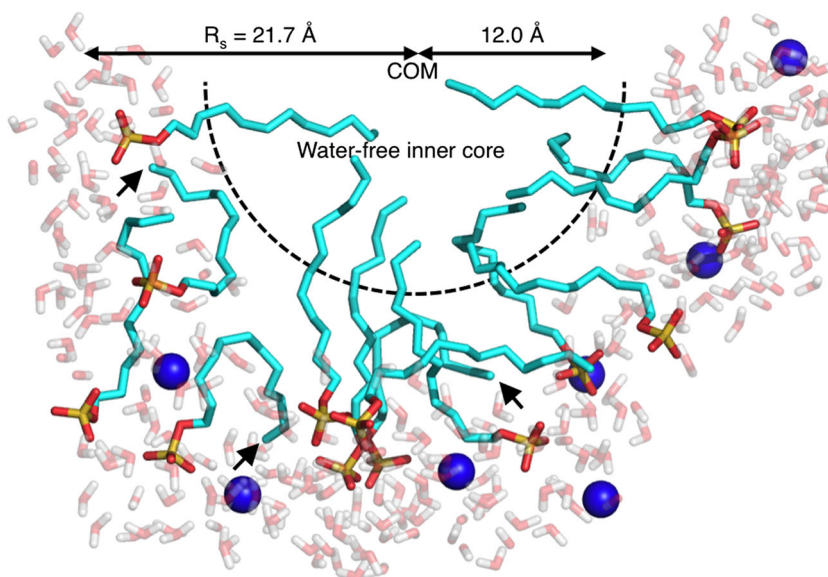
corresponding to the sodium ions distribution (black line, a and b) are both located between two hydration shells (dashed line, 1 and 2 or 3 and 4). Again, this is in agreement with previous MD simulations [15, 21] where the counterions could be coordinated (i) either in a tetrahedral pocket formed by the non-charged oxygen (OA) and two oxygen's of the headgroup (OM), (ii) or by the three negatively charged oxygen atoms of the sulfate headgroups.

The CG model agrees with the AA and UA models by showing four shells of hydration (Fig. 5c, bold line) and three shells of ions (dashed line) around the headgroup. However, contrary to the AA and UA models where each atom from the headgroup is explicitly characterized, the CG representation merges them all in a unique particle avoiding specific interactions between water molecules and ester-type (OA) or sulfonate (OM) oxygen atoms.

Conclusions

SDS is a well-known anionic detergent widely used in both experimental and theoretical investigations. However, the previously published SDS MD simulations are limited due to the description of the SDS molecule based on general parameter sets that are different according to the resolutions.

In that context, we here proposed more coherent sets of parameters for the SDS molecules at CG, UA, and AA resolutions based on a QM-optimized structure. Firstly, we attributed ideal bond lengths, angles, dihedrals, and partial charges obtained from the QM-optimized molecule to the three models. By then comparing our newly described parameters to reference SDS models widely used in simulations, we observed that our new set lead to a more consistent description of the molecule at the different resolutions. Then, SDS micelles were accurately built and MD simulations were performed at three different resolutions in order to compare the respective ability of QM-optimized AA, UA, and CG SDS parameters to properly describe the dynamic behavior of the preformed micelle in water. While all three models present the same macromolecular properties (size, shape, and accessible surface) perfectly matching previous experimental and theoretical results, the attribution of more representative parameters for SDS leads to the reproduction of the specific interactions of the detergent inside and outside the micelle. Indeed, whatever the resolution, the SDS micellar properties are well in line with previous experimental and theoretical results, validating our systematically QM-derived set of parameters.

These coherent sets of parameters describing the AA, UA, and CG SDS molecule could now be used to investigate the SDS-protein interactions at multiscale resolutions.

References

1. Shaw BF, Schneider GF, Arthanari H et al (2011) Complexes of native ubiquitin and dodecyl sulfate illustrate the nature of hydrophobic and electrostatic interactions in the binding of proteins and surfactants. J Am Chem Soc 133:17681–17695
2. Shaw BF, Schneider GF, Whitesides GM (2012) Effect of surfactant hydrophobicity on the pathway for unfolding of ubiquitin. J Am Chem Soc 134:18739–18745
3. Hu W, Liu J, Luo Q et al (2011) Elucidation of the binding sites of sodium dodecyl sulfate to β-lactoglobulin using hydrogen/deuterium exchange mass spectrometry combined with docking simulation. Rapid Commun Mass Spectrom 25:1429–1436
4. Liu R, Bu W, Xi J et al (2012) Beyond the detergent effect: a binding site for sodium dodecyl sulfate (SDS) in mammalian apoferritin. Acta Crystallogr D Biol Crystallogr 68:497–504
5. Tian J, Sethi A, Anunciado D et al. (2012) Characterization of a disordered protein during micellation: interactions of α-synuclein with sodium dodecyl sulfate. J Phys Chem B 116:4417–4424
6. Hayashi S, Ikeda S (1980) Micelle size and shape of sodium dodecyl sulfate in concentrated NaCl solutions. J Phys Chem 84:744–751
7. Quina FH, Preto R, Bales BL (1995) Growth of sodium dodecyl sulfate micelles with detergent concentration. J Phys Chem 99:17028–17031
8. Hassan PA, Fritz G, Kaler EW (2003) Small angle neutron scattering study of sodium dodecyl sulfate micellar growth driven by addition of a hydrotropic salt. J Colloid Interface Sci 257:154–162
9. Chen J, Su T, Mou CY (1986) Size of sodium dodecyl sulfate micelle in concentrated salt solutlons. J Phys Chem 90:2418–2421
10. Corti M, Degiorgio V (1981) Quasi-elastic light scattering study of intermicellar interactions in aqueous sodlum dodecyl sulfate solutions. J Phys Chem 85:711–717
11. Sharma VK, Mitra S, Verma G et al. (2010) Internal dynamics in SDS micelles: neutron scattering study. J Phys Chem B 114:17049–17056
12. Itri D, Amaral LQ (1991) Distance distribution function of sodium dodecyl sulfate micelles by X-ray scattering. J Phys Chem 95:423–427
13. Hammouda B (2013) Temperature effect on the nanostructure of SDS micelles in water. J Res Natl Inst Stand Technol 118:151–167
14. Mcmanus HJD, Kang YS, Kevan L (1992) Electron spin resonance, electron spin echo, and electron nuclear double resonance studies of the photoreduction yield of a series of alkylmethyiviologens in sodium dodecyl sulfate and dodecyltrimethylammonium chloride micelles : effect of the alkyl cha. J Phys Chem 96:5622–5628
15. Behera K, Pandey S (2007) Modulating properties of aqueous sodium dodecyl sulfate by adding hydrophobic ionic liquid. J Colloid Interface Sci 316:803–814
16. Jalili S, Akhavan M (2009) A coarse-grained molecular dynamics simulation of a sodium dodecyl sulfate micelle in aqueous solution. Colloids Surf A Physicochem Eng Asp 352:99–102
17. Sangwai A, Sureshkumar R (2011) Coarse-grained molecular dynamics simulations of the sphere to rod transition in surfactant micelles. Langmuir 27:6628–6638
18. Levine BG, LeBard DN, DeVane R et al. (2011) Micellization Studied by GPU-Accelerated Coarse-Grained Molecular Dynamics. J Chem Theory Comput 7:4135–4145
19. Jalili S, Akhavan M (2011) Study of the Alzheimer's Aβ40 peptide in SDS micelles using molecular dynamics simulations. Biophys Chem 153:179–186
20. Bruce CD, Berkowitz ML, Perera L, Forbes MDE (2002) Molecular dynamics simulation of sodium dodecyl sulfate micelle in water: micellar structural characteristics and counterion distribution. J Phys Chem B 106:3788–3793
21. Bruce CD, Senapati S, Berkowitz ML et al (2002) Molecular dynamics simulations of sodium dodecyl sulfate micelle in water: the behavior of water. J Phys Chem B 106:10902–10907

22. Gao J, Ge W, Hu G, Li J (2005) From homogeneous dispersion to micelles-a molecular dynamics simulation on the compromise of the hydrophilic and hydrophobic effects of sodium dodecyl sulfate in aqueous solution. Langmuir 21:5223–5229

23. Yan H, Cui P, Liu C, Yuan S (2012) Molecular dynamics simulation of pyrene solubilized in a sodium dodecyl sulfate micelle. Langmuir 28:4931–4938

24. Sammalkorpi M, Karttunen M, Haataja M (2007) Structural properties of ionic detergent aggregates: a large-scale molecular dynamics study of sodium dodecyl sulfate. J Phys Chem B 111:11722–11733

25. Yan H, Yuan S-L, Xu G-Y, Liu C-B (2010) Effect of Ca2+ and Mg2+ ions on surfactant solutions investigated by molecular dynamics simulation. Langmuir 26:10448–10459

26. Mackerell AD (1995) Molecular dynamics simulation analysis of a sodium dodecyl sulfate micelle in aqueous solution: decreased fluidity of the micelle hydrocarbon interior. J Phys Chem 99:1846–1855

27. Langham AA, Waring AJ, Kaznessis YN (2007) Comparison of interactions between beta-hairpin decapeptides and SDS/DPC micelles from experimental and simulation data. BMC Biochem 8:11, 1

28. Comba P, Remenyi R (2003) Inorganic and bioinorganic molecular mechanics modeling - the problem of the force field parameterization. Coord Chem Rev 238–239:9–20

29. Oostenbrink C, Villa A, Mark AE, van Gunsteren WF (2004) A biomolecular force field based on the free enthalpy of hydration and solvation: the GROMOS force-field parameter sets 53A5 and 53A6. J Comput Chem 25:1656–1676

30. Brocos P, Mendoza-Espinosa P, Castillo R et al (2012) Multiscale molecular dynamics simulations of micelles: coarse-grain for self-assembly and atomic resolution for finer details. Soft Matter 8: 9005

31. Kraft JF, Vestergaard M, Schiøtt B, Thøgersen L (2012) Modeling the self-assembly and stability of DHPC micelles using atomic resolution and coarse grained MD simulations. J Chem Theory Comput 8: 1556–1569

32. Stansfeld PJ, Sansom MSP (2011) From coarse grained to atomistic: a serial multiscale approach to membrane protein simulations. J Chem Theory Comput 7:1157–1166

33. Bessonov K, Vassall KA, Harauz G (2013) Parameterization of the proline analogue Aze (azetidine-2-carboxylic acid) for molecular dynamics simulations and evaluation of its effect on homo-pentapeptide conformations. J Mol Graph Model 39:118–125

34. Cao Z, Liu L, Zhao L et al (2013) Comparison of the structural characteristics of Cu(2+)-bound and unbound α-syn12 peptide

35. Soares T, Hünenberger PH, Kastenholz MA et al (2005) An improved nucleic acid parameter set for the GROMOS force field. J Comput Chem 26:725–737

36. Liu X, Zhang S, Zhou G et al (2006) New force field for molecular simulation of guanidinium-based ionic liquids. J Phys Chem B 110: 12062–12071

37. Marrink SJ, Risselada HJ, Yefimov S et al (2007) The MARTINI force field: coarse grained model for biomolecular simulations. J Phys Chem B 111:7812–7824

38. Terakawa T, Takada S (2014) RESPAC: method to determine partial charges in coarse-grained protein model and its application to DNA-binding proteins. J Chem Theory Comput 10:711–721

39. Martínez L, Andrade R, Birgin EG, Martínez JM (2009) Packmol: a package for building initial configurations for molecular dynamics simulations. J Comput Chem 30:2157–2164

40. Hess B, Kutzner C, van der Spoel D, Lindahl E (2008) GROMACS 4: algorithms for highly efficient, load-balanced, and scalable molecular simulation. J Theory Comput 4:435–447

41. Sanders SA, Sammalkorpi M, Panagiotopoulos AZ (2012) Atomistic simulations of micellization of sodium hexyl, heptyl, octyl, and nonyl sulfates. J Phys Chem B 116:2430–2437

42. Berendsen HJC, Postma JPM, van Gunsteren WF et al (1984) Molecular dynamics with coupling to an external bath. J Chem Phys 81:3684–3690

43. Humphrey W, Dalke A, Schulten K (1996) VMD: Visual molecular dynamics. J Mol Graph 14:33–38

44. Bogusz S, Venable RM, Pastor RW (2000) Molecular dynamics simulations of octyl glucoside micelles: structural properties. J Phys Chem B 104:5462–5470

45. Yoshii N, Okazaki S (2007) A molecular dynamics study of structure and dynamics of surfactant molecules in SDS spherical micelle. Condens Matter Phys 10:573–578

46. Salaniwal S, Cui ST, Cochran HD, Cummings PT (2001) Molecular simulation of a dichain surfactant/water/carbon dioxide system. 1. Structural properties of aggregates. Langmuir 17:1773–1783

47. Stephany SM, Kole TM, Fisch MR (1994) Light scattering study of the effects of 1-pentanol on solutions of sodium dodecyl sulfate in NaCl-H20 solutions. J Phys Chem 98:11126–11128

48. Morisada S, Shinto H (2010) Implicit solvent model simulations of surfactant self-assembly in aqueous solutions. J Phys Chem B 114: 6337–6343